Supplement of Geosci. Model Dev., 17, 3259–3277, 2024
https://doi.org/10.5194/gmd-17-3259-2024-supplement

Geoscientific Model Development
Open Access
EGU

Supplement of

The regional climate–chemistry–ecology coupling model RegCM-Chem (v4.6)–YIBs (v1.0): development and application

Nanhong Xie et al.

Correspondence to: Tijian Wang (tjwang@nju.edu.cn)

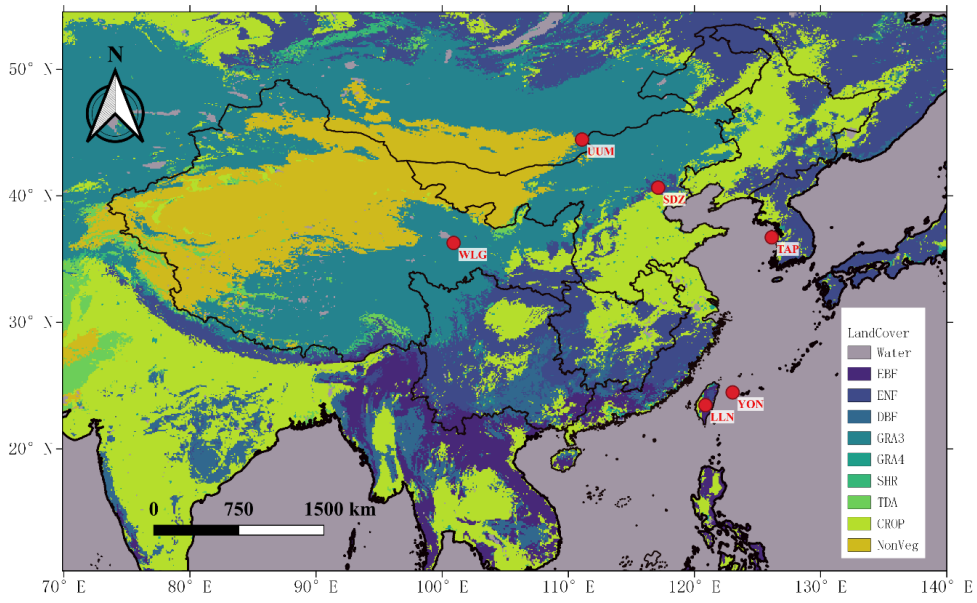

Figure S1. Distribution map of surface vegetation types in the simulated area. Evergreen broad-leaved forest (EBF), evergreen coniferous forest (ENF), deciduous broad-leaved forest (DBF), C3 grassland (GRA3), C4 grassland (GRA4), shrub forest (SHR), tundra (TDA), crops (CROP). The red circles indicate the locations of CO_2 observation sites.

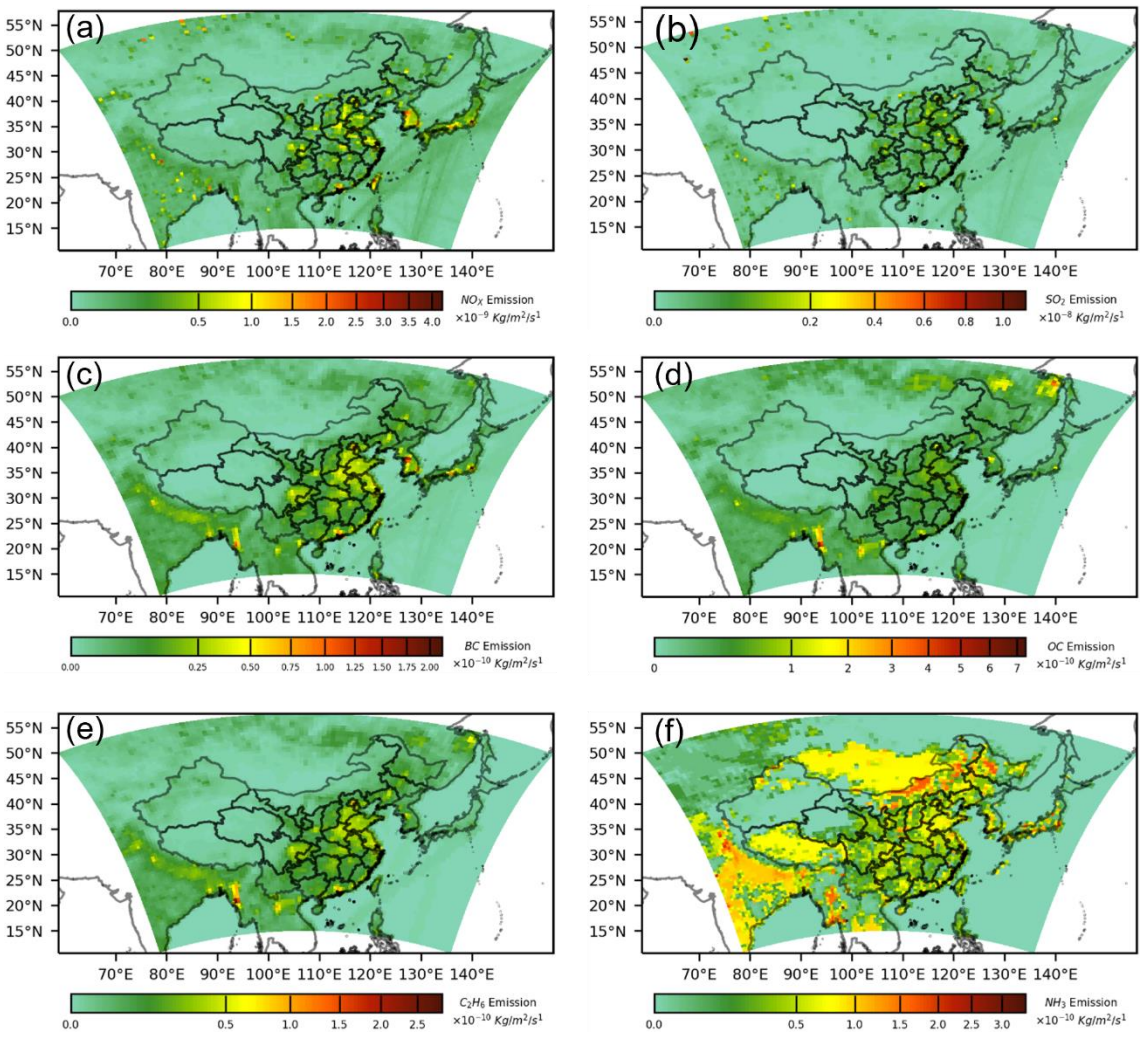

Figure S2. Emission fluxes of main pollutants (NO_X(a), SO_2(b), BC(c), OC(d), C_2H_6(e), NH_3(f)) in the simulation area. Units: Kg m^{-2} s^{-1}.

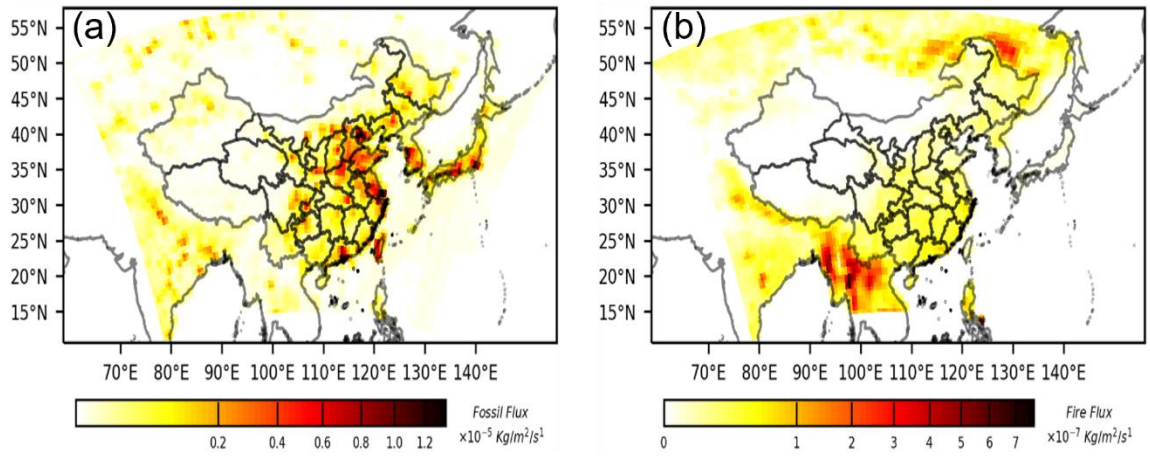

Figure S3. Modeling regional CO_2 emission fluxes from fossil fuel(a) and biomass combustion(b). Units: Kg m^{-2} s^{-1}.

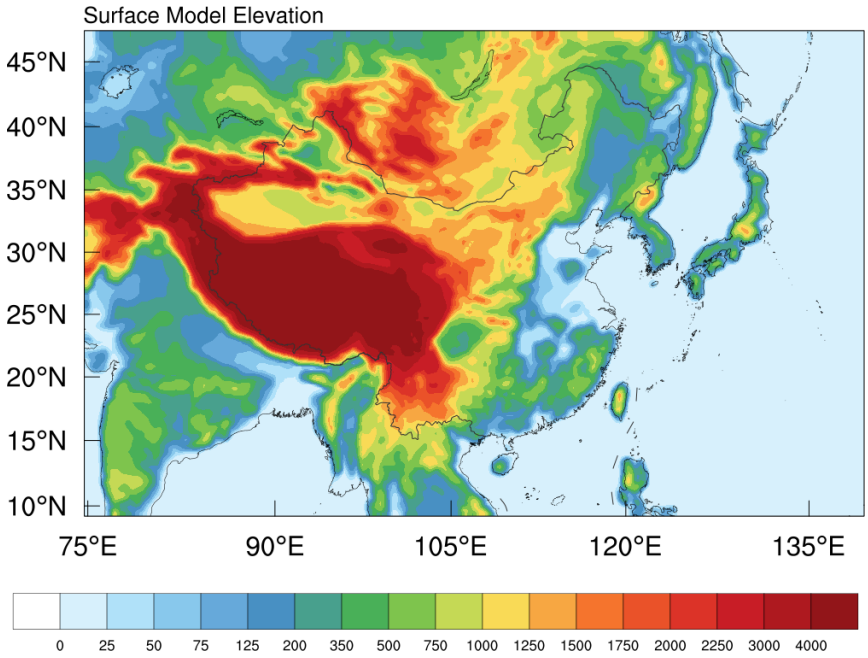

Figure S4. The modelling domain applied and Topographic Elevation (Units: m) in this study.

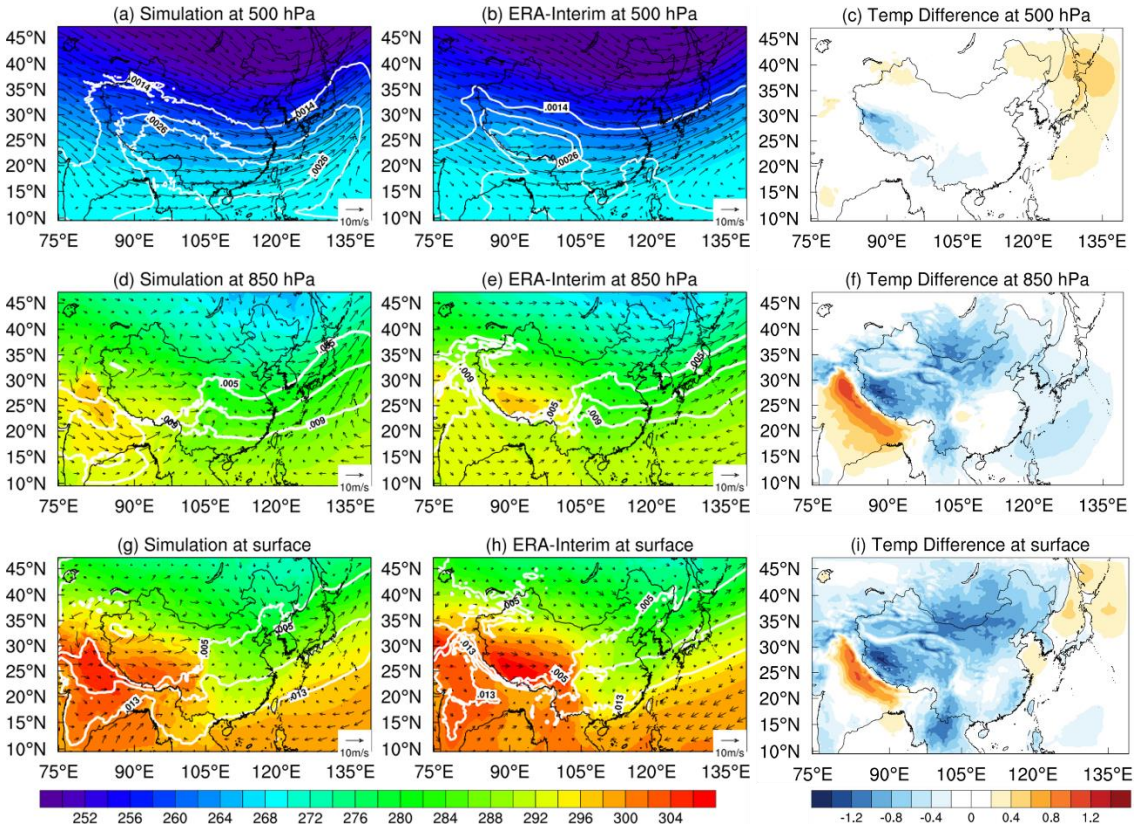

Figure S5. Temperature (color-filled; units: K), specific humidity (contours; units: kg kg^{-1}) and wind field (streamlines; units: m s^{-1}) in 2016 at 500 hPa (a, b), 850 hPa (d, e) and near surface (g, h) for the model simulation (a, d, g) and ERA-Interim data (b, e, h). The column on the far right shows the differences between simulated and observed temperature at 500hPa (c), 850hPa (f), and surface (i). The differences are simulation minus observation.

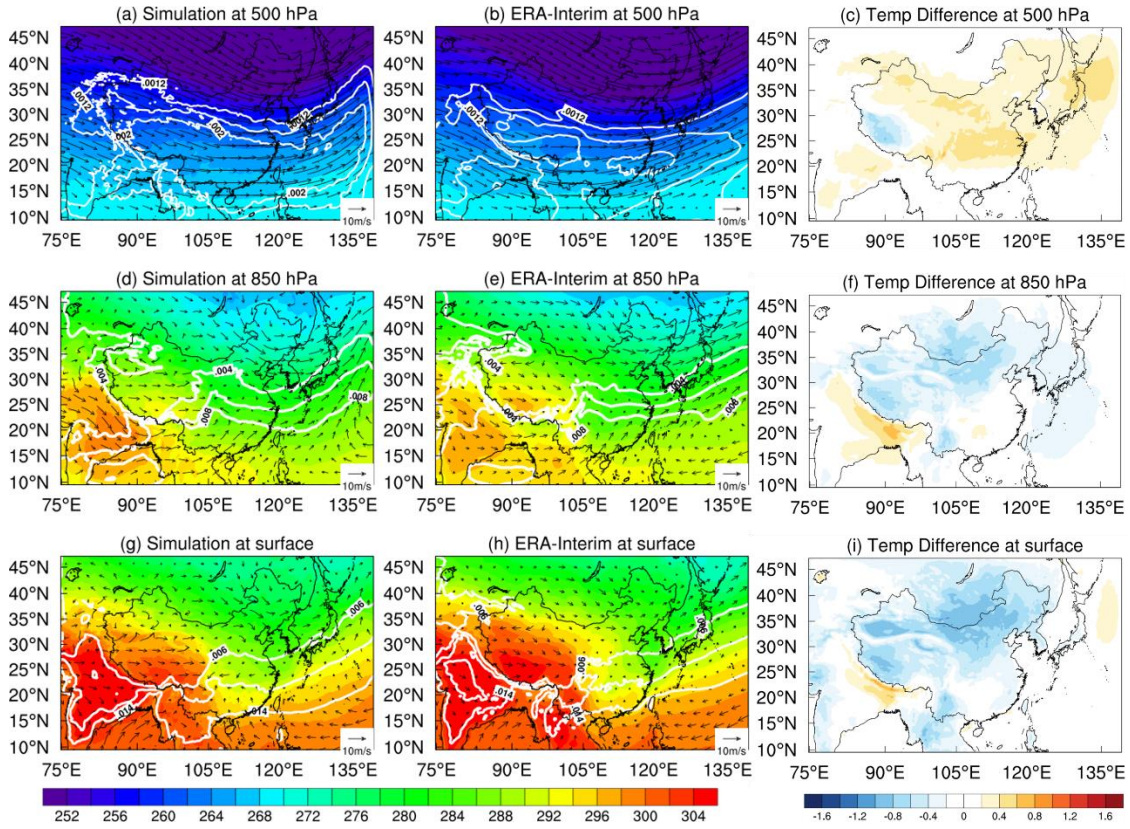

Figure S6. Spring average temperature (color-filled; units: K), specific humidity (contours; units: kg kg^{-1}) and wind field (streamlines; units: m s^{-1}) in 2016 at 500 hPa (a, b), 850 hPa (d, e) and near surface (g, h) for the model simulation (a, d, g) and ERA-Interim data (b, e, h). The column on the far right shows the differences between simulated and observed temperature at 500hPa (c), 850hPa (f), and surface (i). The differences are simulation minus observation. The months we defined as spring include March, April and May.

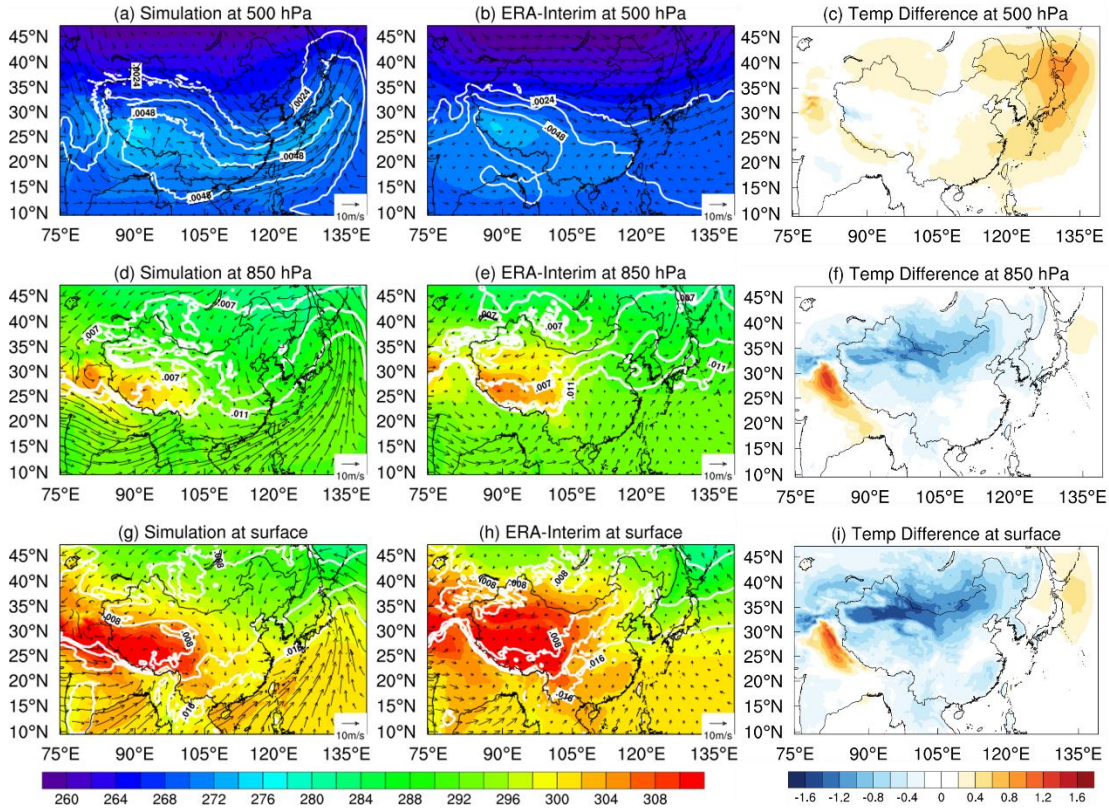

Figure S7. Summer average temperature (color-filled; units: K), specific humidity (contours; units: kg kg^{-1}) and wind field (streamlines; units: m s^{-1}) in 2016 at 500 hPa (a, b), 850 hPa (d, e) and near surface (g, h) for the model simulation (a, d, g) and ERA-Interim data (b, e, h). The column on the far right shows the differences between simulated and observed temperature at 500hPa (c), 850hPa (f), and surface (i). The differences are simulation minus observation. The months we define as summer include June, July and August.

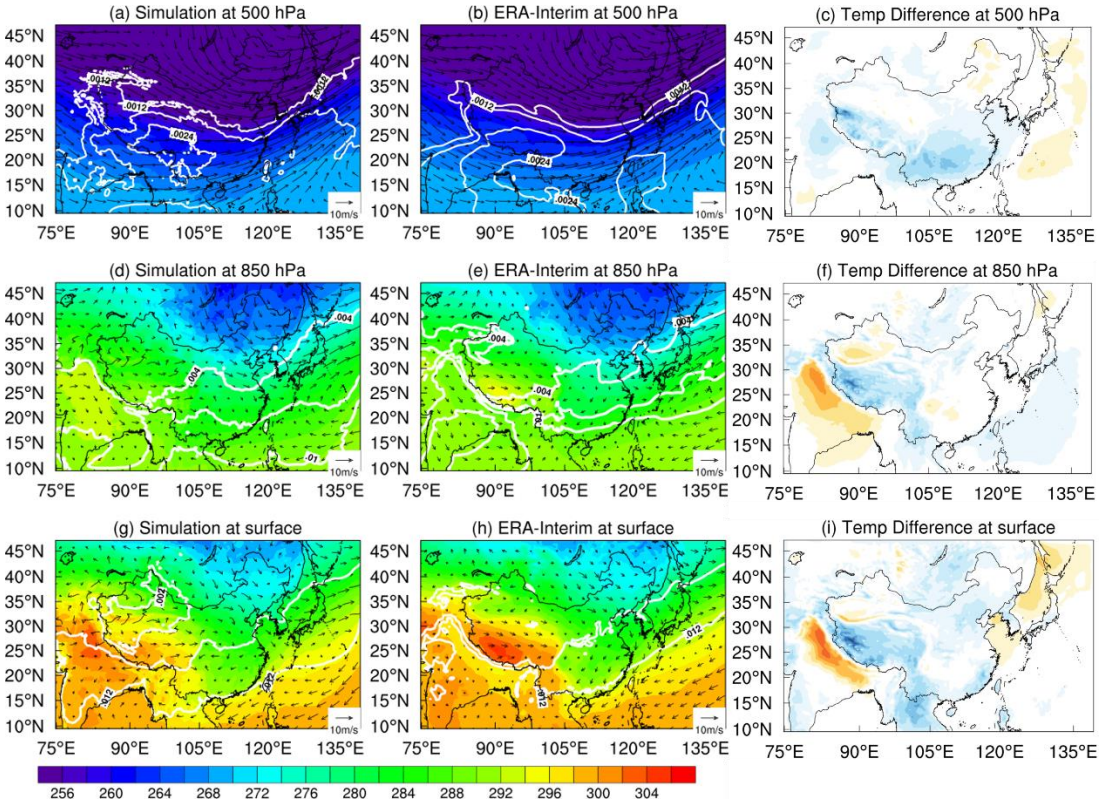

Figure S8. Autumn average temperature (color-filled; units: K), specific humidity (contours; units: kg kg^{-1}) and wind field (streamlines; units: m s^{-1}) in 2016 at 500 hPa (a, b), 850 hPa (d, e) and near surface (g, h) for the model simulation (a, d, g) and ERA-Interim data (b, e, h). The column on the far right shows the differences between simulated and observed temperature at 500hPa (c), 850hPa (f), and surface (i). The differences are simulation minus observation. The months we define as autumn include September, October and November.

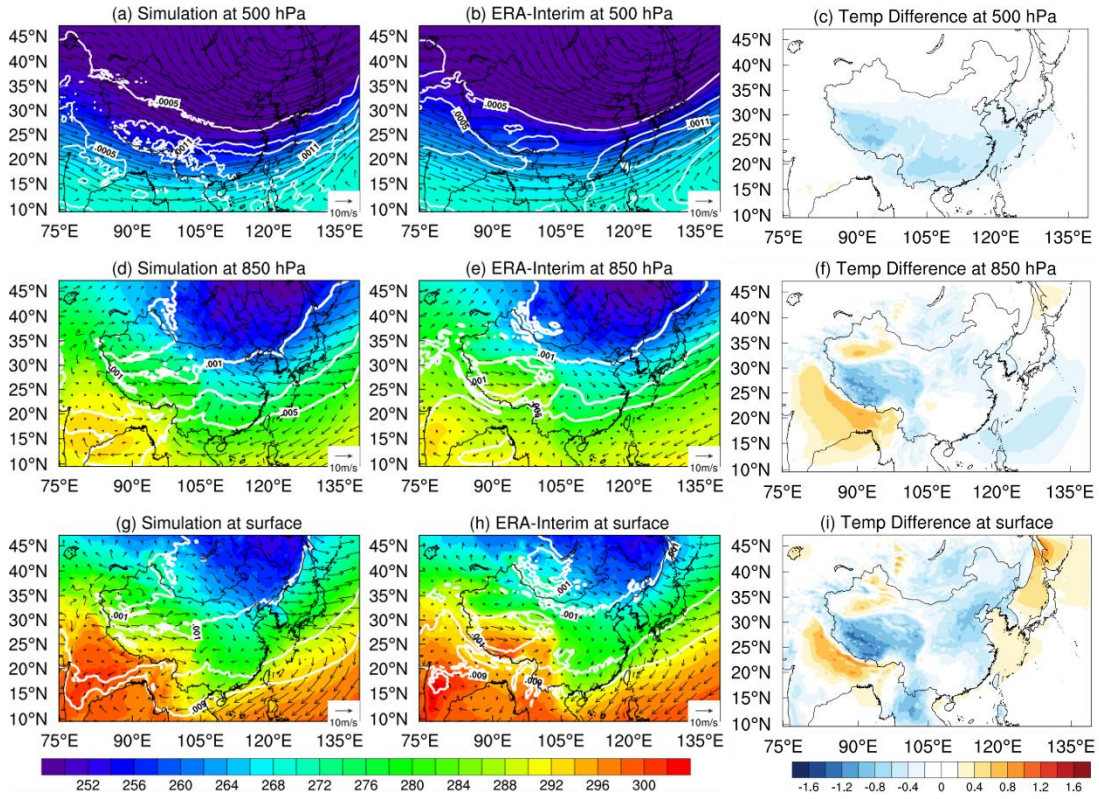

Figure S9. Winter average temperature (color-filled; units: K), specific humidity (contours; units: kg kg^{-1}) and wind field (streamlines; units: m s^{-1}) in 2016 at 500 hPa (a, b), 850 hPa (d, e) and near surface (g, h) for the model simulation (a, d, g) and ERA-Interim data (b, e, h). The column on the far right shows the differences between simulated and observed temperature at 500hPa (c), 850hPa (f) and surface (i). The differences are simulation minus observation. The months we define as winter include January, February and December.

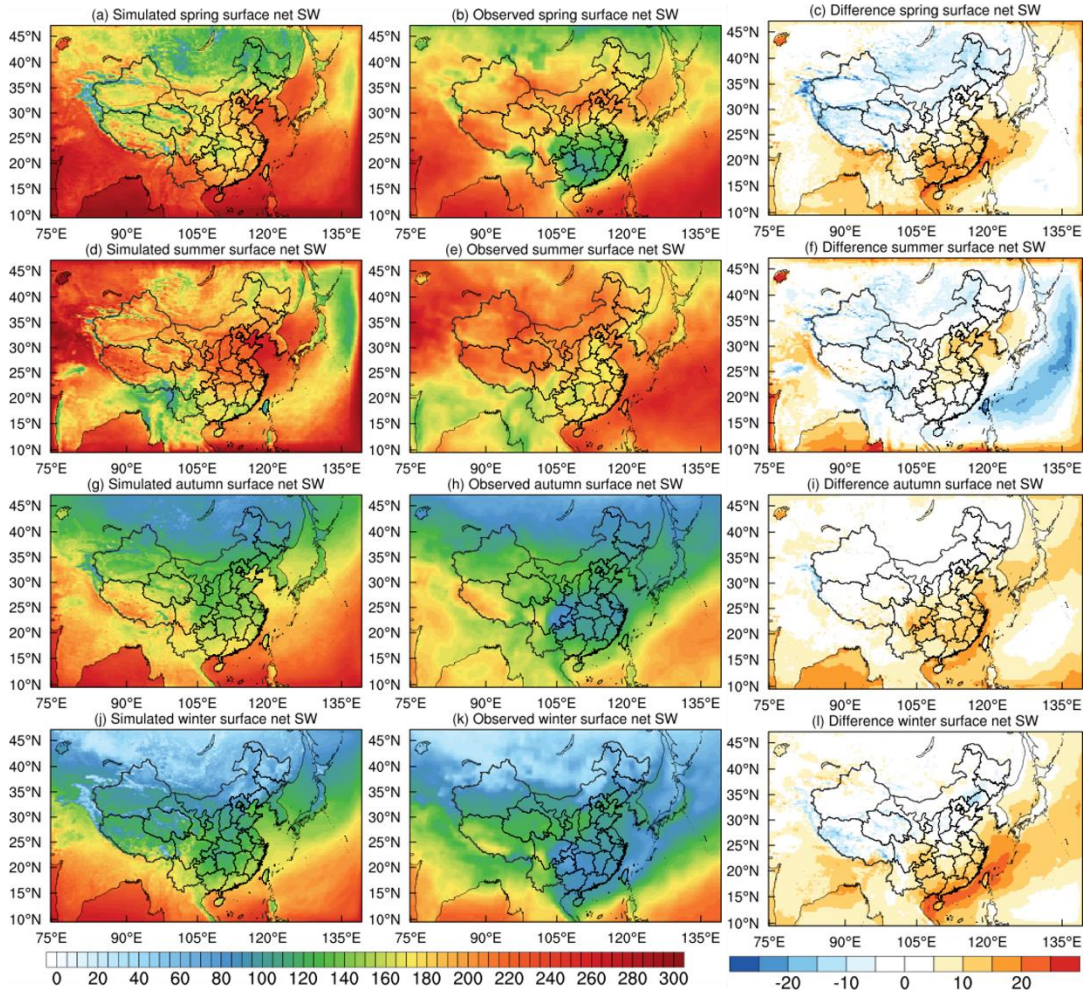

Figure S10. Spring (a, b), summer (d, e), autumn (g, h), winter (j, k) four season model simulations (a, d, g, j) and satellite retrieval (b, e, h, k) in 2016 surface net shortwave radiation flux. The column on the far right shows the difference between simulations and observations for spring(c), summer(f), autumn(i), and winter(l). The differences are simulation minus observation. Units: W m^{-2}.

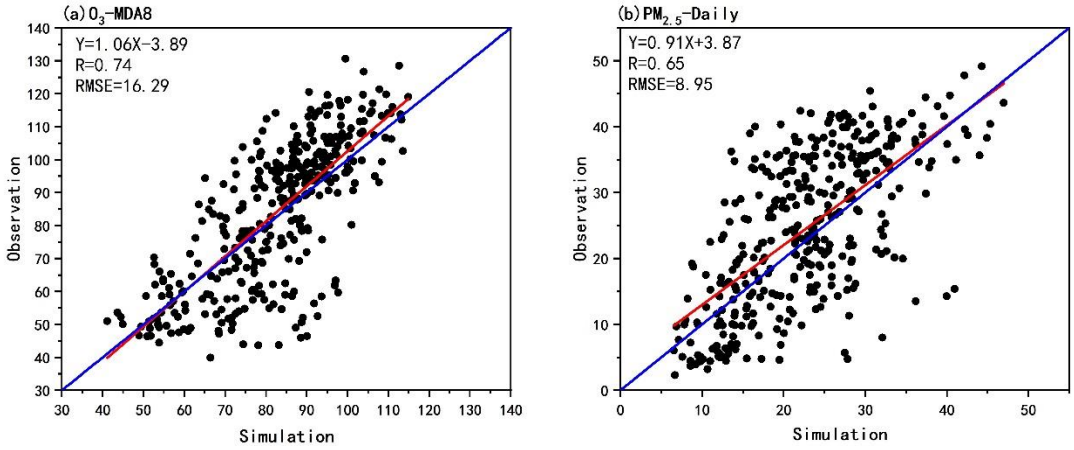

Figure S11. Scatter plot of simulated and observed for O_3 (a) and $PM_{2.5}$(b) Units: μg m^{-3}

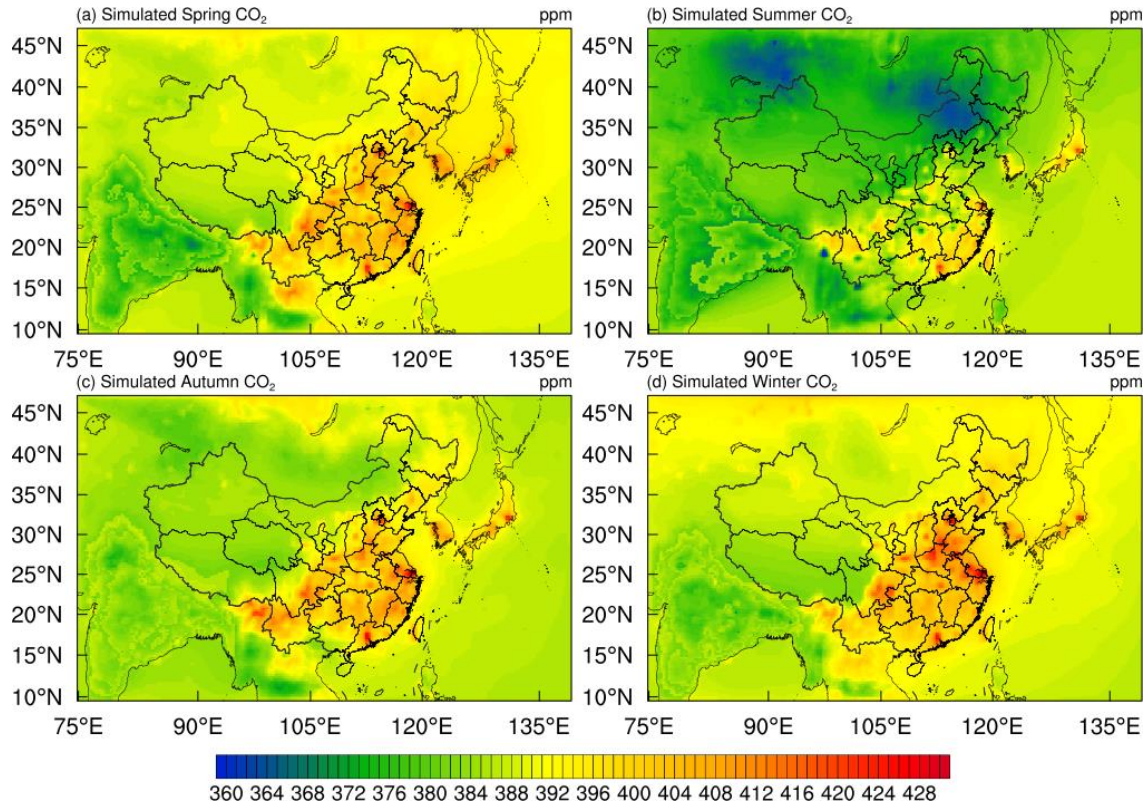

Figure S12. Spatial distribution of CO_2 simulated by model of spring(a), summer(b), autumn(c) and winter(d) in 2016. Units: ppm

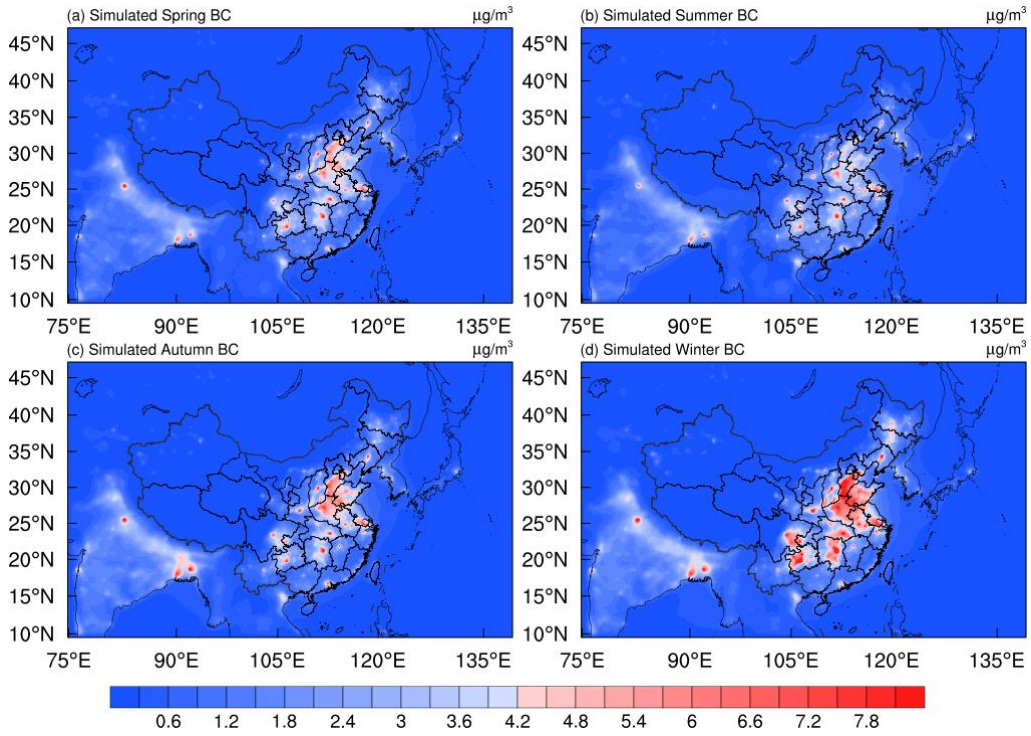

Figure S13. Spatial distribution of BC simulated by four season models of spring(a), summer(b), autumn(c) and winter(d) in 2016. Units: μg m^{-3}

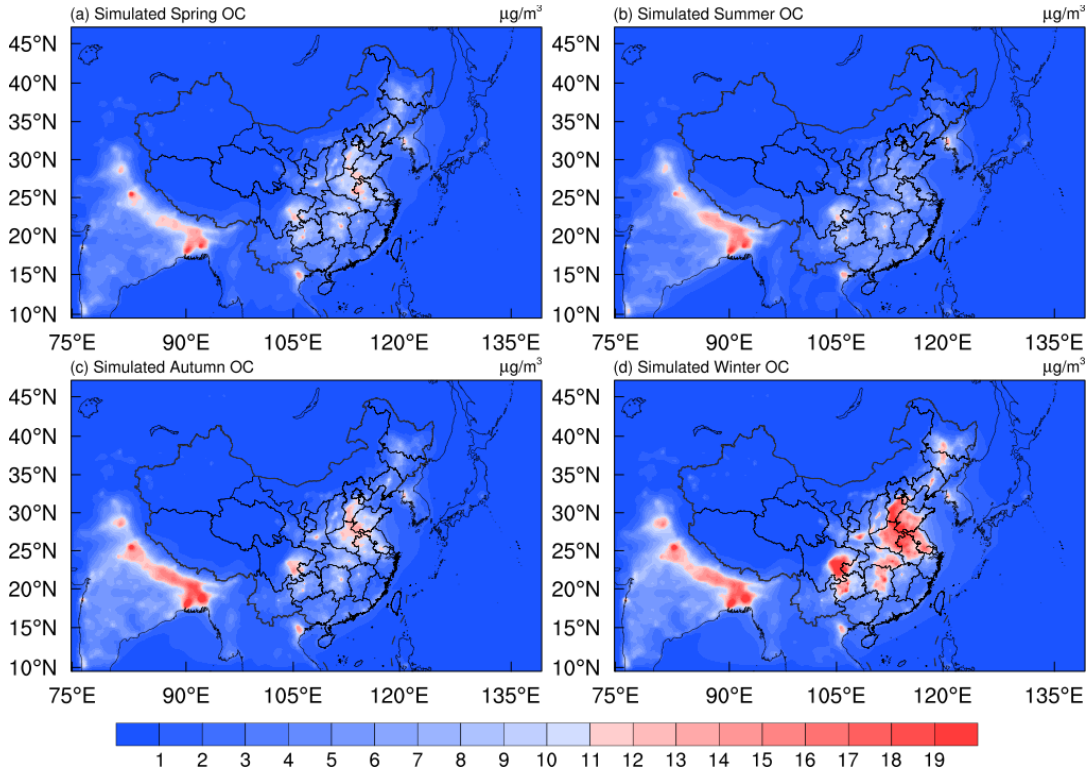

Figure S14. Spatial distribution of OC simulated by four season models of spring(a), summer(b), autumn(c) and winter(d) in 2016. Units: μg m^{-3}

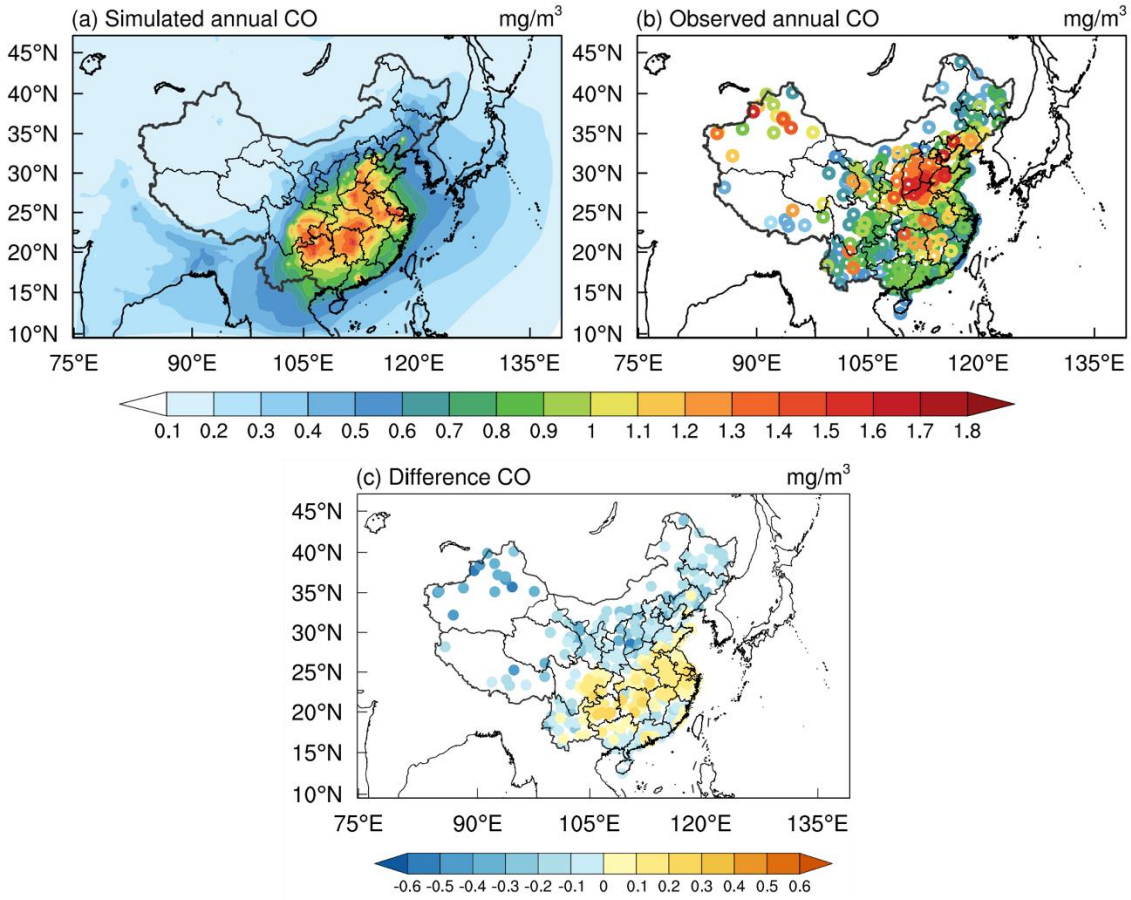

Figure S15. Comparisons of simulations (a) and observations (b) and their differences (c) for CO across China. Colored circles show station observations. The differences are simulation minus observation. Units: mg m^{-3}.

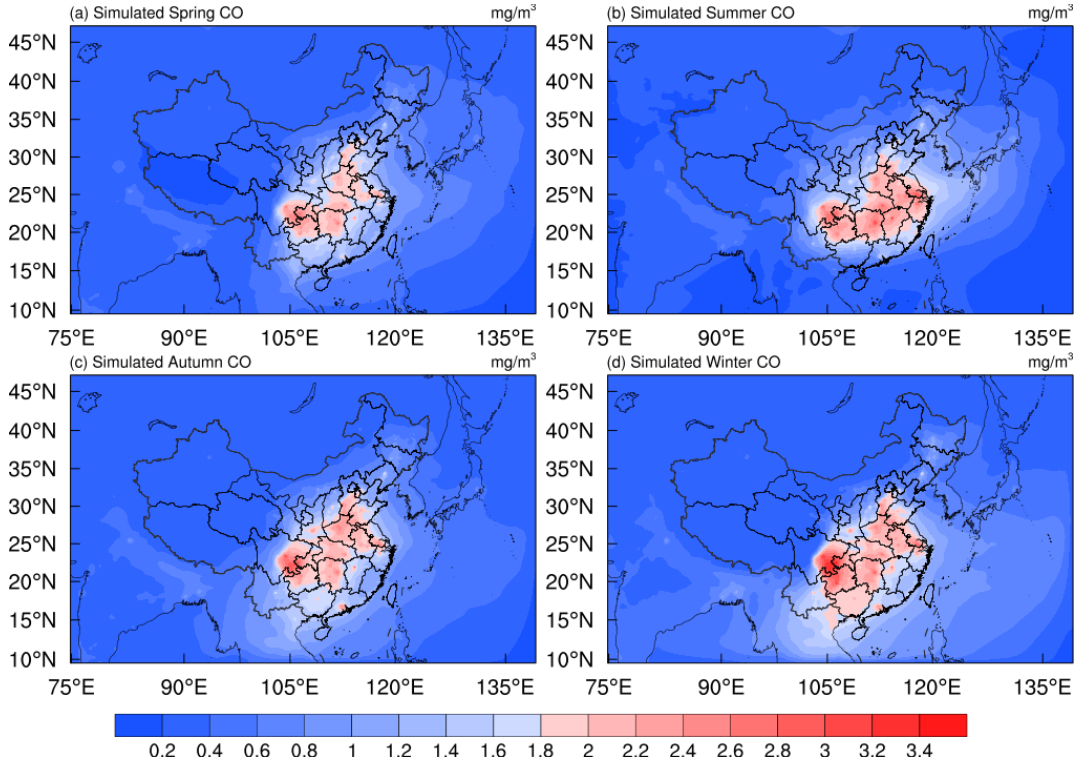

Figure S16. Spatial distribution of CO simulated by four season models of spring(a), summer(b), autumn(c) and winter(d) in 2016. Units: mg m^{-3}

Table S1. Statistical metrics for surface O_3 and $PM_{2.5}$ concentration

Variables	R	MB	ME	NMB	NME	RMSE
O_3_MDA8	0.74	-1.47	11.61	0.0235	0.1577	16.29
$PM_{2.5}$_Daily	0.65	-1.80	7.21	0.1380	0.4211	8.95

(Abbreviated meaning: correlation coefficients (R), mean biases(MB), mean error (ME), normal mean biases (NMB), normal mean error (NME), and root mean square error (RMSE). MB, ME and RMSE units: $\mu g\ m^{-3}$)

Table S2. Comparison between Observation and simulation carbon fluxes

Variables	R	MB	ME	RMSE
GPP	0.91	0.13	0.22	0.40
NPP	0.87	0.05	0.12	0.22

(The abbreviation definitions R, MB, ME, and RMSE are consistent with Table S1. MB, ME and RMSE units: $Kg\ C\ m^{-2}\ year^{-1}$)